Effects of the Arrangement of a Distal Catalytic Residue on Regioselectivity and Reactivity in the Coupled Oxidation of Sperm Whale Myoglobin Mutants

Tatsuya Murakami,[†] Isao Morishima,*[,†] Toshitaka Matsui,[‡] Shin-ichi Ozaki,[‡,§] Isao Hara,[‡] Hui-Jun Yang,[‡] and Yoshihito Watanabe*[,‡,§]

Contribution from the Department of Molecular Engineering, Graduate School of Engineering, Kyoto University, Kyoto 606-01, Japan, Department of Structural Molecular Science, The Graduate University for Advanced Studies, Okazaki, Myodaiji 444, Japan, and Institute for Molecular Science, Okazaki, Myodaiji 444, Japan

Received September 25, 1998

Abstract: The coupled oxidations of sperm whale myoglobin (Mb) mutants are performed to examine active site residues controlling the regiospecific heme degradation. HPLC analysis of biliverdin isomers shows that L29H/H64L Mb almost exclusively gives biliverdin IXγ, although H64L and wild-type Mb mainly afford the α-isomer. Relocation of the distal histidine at the 43 and 107 positions increases the amount of γ-isomer to 44 and 22%, respectively. Interestingly, the increase in the ratio of γ-isomer is also observed by a single replacement of either His-64 with Asp or Phe-43 with Trp. It appears that the polarity of the active site as well as hydrogen bonding between oxygen molecule bound to the heme iron and His or Trp is important in controlling the regioselectivity. The results of coupled oxidation kinetics, autoxidation kinetics, and redox potential of the Fe^{3+}/Fe^{2+} couple are discussed with regard to their implications for the active site and mechanism of heme oxygenase.

Introduction

Heme oxygenase is a central monooxygenase of the heme catabolism[1] and forms a stoichiometric complex with protoheme IX.[2] The enzyme utilizes electrons and molecular oxygen for the regioselective heme degradation to yield α-biliverdin and carbon monoxide (CO) through three sequential oxygenase reactions. The formation of ferrous oxy heme is followed by hydroxylation of the α-*meso*-carbon presumably via ferric hydroperoxide complex ($Fe^{3+}-OOH$).[3] The release of CO leads to verdoheme, which is converted to biliverdin (Scheme 1). The *meso*-hydroxylation is a key step for the regiospecific ring opening of the tetrapyrrole macrocycle.

Torpey et al. recently examined the regioselectivity of the oxidized products of methylmesoheme and formylmesoheme by heme oxygenase and suggested that the regiochemistry of the reaction could be primarily controlled by electronic rather than steric effects.[4] On the other hand, recent resonance Raman studies suggested that the O_2-bound heme−heme oxygenase complex had a highly bent structure of the coordinated oxygens whose terminal oxygen atom was in van der Waals contact with the α-*meso*-carbon of the porphyrin ring.[5] Furthermore, ESR studies of the O_2-bound cobalt heme−heme oxygenase complex provide evidence for hydrogen bonding of a distal residue to the bound O_2 on the basis of an isotope-sensitive signal in both ^1H_2O and ^2H_2O.[6] Therefore, a specific orientation of the bound O_2 toward the α-*meso*-carbon induced by the hydrogen bonding may also be important for the regioselectivity.

Myoglobin (Mb) has a neutral histidine ligand as in the heme−heme oxygenase complex[7] and exhibits a heme oxygenase type regiospecific tetrapyrrole ring opening.[8] The degradation of heme by Mb, so-called coupled oxidation, can be performed in the presence of a large excess of ascorbate.[9] Although the mechanism of heme degradation by Mb may not be the same as that by heme oxygenase, the ring opening proceeds preferentially at the α-*meso*-carbon. The specific oxidation of the α-*meso* position is expected on the basis of its crystal structure of oxy Mb (Figure 1).[10] The molecular oxygen bound to the heme iron is forced to bend between the α- and β-*meso*-carbons, and the bound O_2 is stabilized by the hydrogen bond interaction with the distal histidine. Furthermore, the access of the γ-*meso* position is restricted by the distal histidine. In

† Kyoto University.
‡ The Graduate University for Advanced Studies.
§ Institute for Molecular Science.
* To whom correspondence should be addressed. Telephone: +81-564-54-7430. Fax: +81-564-54-2254. E-mail: yoshi@ims.ac.jp.

(1) (a) Tenhunen, R.; Marver, H. S.; Schmid, R. J. *Proc. Natl. Acad. Sci. U.S.A.* **1968**, *61*, 748. (b) Tenhunen, R.; Marver, H. S.; Schmid, R. *J. Biol. Chem.* **1969**, *244*, 6388−6394.
(2) Yoshida, T.; Kikuchi, G. *J. Biol. Chem.* **1978**, *253*, 4224−4229.
(3) (a) Noguchi, M.; Yoshida, T.; Kikuchi, G. *J. Biochem. (Tokyo)* **1983**, *93*, 1027−1036. (b) Wilks, A.; Torpey, J.; Ortiz de Montellano, P. R. *J. Biol. Chem.* **1994**, *269*, 29553−29556.
(4) (a) Torpey, J.; Lee, A. D.; Smith, K. M.; Ortiz de Montellano, P. R. *J. Am. Chem. Soc.* **1996**, *118*, 9172−9173. (b) Torpey, J.; Ortiz de Montellano, P. R. *J. Biol. Chem.* **1996**, *271*, 26067−26073. (c) Torpey, J.; Ortiz de Montellano, P. R. *J. Biol. Chem.* **1997**, *272*, 22008−22014.
(5) Takahashi, S.; Ishikawa, K.; Takeuchi, N.; Ikeda-Saito, M.; Yoshida, T.; Rousseau, D. L. *J. Am. Chem. Soc.* **1995**, *117*, 6002−6006.
(6) Fujii, H.; Dou, Y.; Zhou, H.; Yoshida, T.; Ikeda-Saito, M. *J. Am. Chem. Soc.* **1998**, *120*, 8251−8252.
(7) (a) Takahashi, S.; Wang, J.; Rousseau, D. L.; Ishikawa, K.; Yoshida, T.; Takeuchi, N.; Ikeda-Saito, M. *Biochemistry* **1994**, *33*, 5531−5538. (b) Sun, J.; Wilks, A.; Ortiz de Montellano, P. R.; Loehr, T. M. *Biochemistry* **1993**, *32*, 14151−14157.
(8) O'Carra, P.; Colleran, E. *FEBS Lett.* **1969**, *5*, 295−298.
(9) Lemberg, R. *Rev. Pure. Appl. Chem.* **1956**, *6*, 1−23.
(10) Phillips, S. E. *J. Mol. Biol.* **1980,** *142*, 531−534.

10.1021/ja9834576 CCC: $18.00
Published on Web 02/24/1999

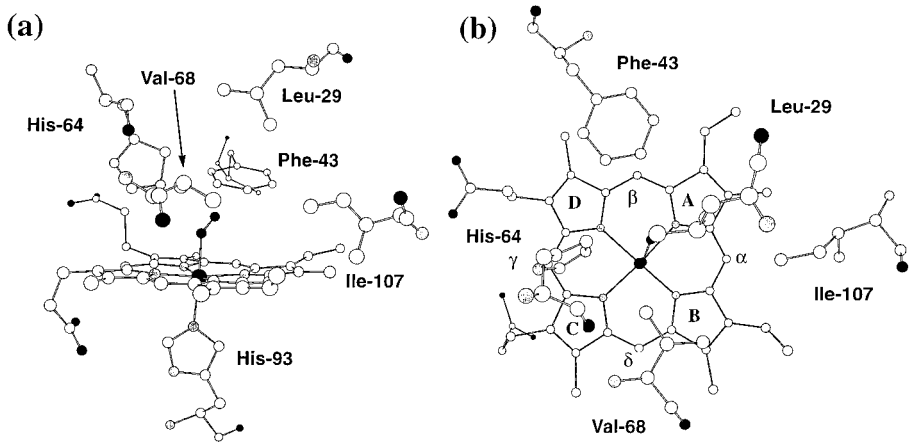

Figure 1. Heme environmental structure of myoglobin. Heme and some selected residues are shown: (a) side view; (b) top view.

Scheme 1. Probable Reaction Sequence of Intermediates in the Heme Oxygenase-Catalyzed Conversion of Heme to Biliverdin

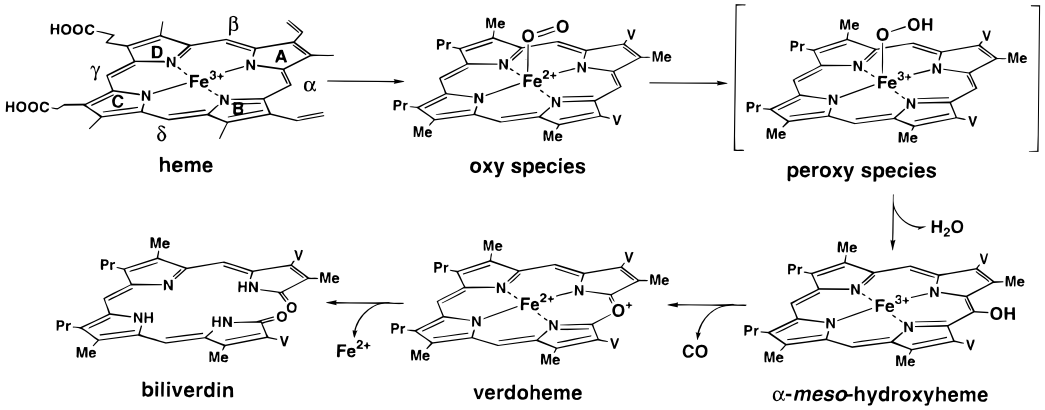

addition, the *β-meso* position is covered with Phe-43. Thus, the steric effect as well as hydrogen bond interaction appears to be important in the regioselective coupled oxidation.

We have recently prepared L29H/H64L[11] and F43H/H64L[12] Mb to mimic the distal site structure of cytochrome *c* peroxidase (C*c*P) and found that F43H/H64L Mb shows the efficient O−O bond cleavage of the peroxy intermediate (Fe^{3+}−OOH), resulting in enhancement of the peroxidase and peroxygenase activity. Since the hydroperoxy species also seems to be involved in the coupled oxidation process (Scheme 1), we have been motivated to examine the regiospecific heme degradation utilizing Mb mutants. While our preliminary work was reported,[13] we describe here details of reactivity and regioselectivity in the coupled oxidation by L29H/H64L, F43H/H64L, I107H/H64L, F43W, F43W/H64L, and H64D Mb.

Experimental Section

Sodium dithionite and sodium ascorbate were purchased from Wako Pure Chemical Industries, Ltd.

Site-Directed Mutagenesis, Expression, and Purification of Mb. Site-directed mutagenesis of Leu-29, Phe-43, and Ile-107 in recombinant sperm whale myoglobin was carried out by using the polymerase chain reaction (PCR) according to a method previously reported.[14]

The His-64→Leu and His-64→Asp replacements were achieved by cassette mutagenesis and confirmed by DNA sequence analysis on a ABI Prism 373 DNA Sequencer (Applied Biosystems). The cassette including desired His-64 substitution and a new silent *Hpa*I restriction site was inserted between the *Bgl*II and *Hpa*I sites. The expression and purification of the mutants were performed according to methods previously described.[14]

Spectroscopy. All spectroscopic measurements were performed in 50 mM sodium phosphate buffer (pH 7.0) unless otherwise stated. Electronic absorption spectra were recorded on a Perkin-Elmer Lambda 19 spectrometer with the samples whose concentrations were adjusted to ca. 5 μM. The coupled oxidation assays were performed in a buffer containing ascorbate (1 mM) at 37 °C. Spectra were recorded (300−850 nm) for 5 h.

Measurements of autoxidation rates of the oxy complexes of wild-type and mutant Mb were made at 37 °C using ca. 5 μM protein in the buffer. The mutants were reduced with an excess amount of sodium dithionite and loaded on a small Sephadex G-25 (Pharmacia) column equilibrated and eluted with CO-saturated 50 mM sodium phosphate buffer, pH 7.0. The resultant CO Mb without any reductant was converted to the oxy Mb by irradiation of a white lamp under an O_2 atmosphere at 0 °C. The oxy complex of wild-type Mb was directly prepared from the ferric Mb by passing the reduced complex by sodium dithionite through a small G-25 column equilibrated and eluted with air-saturated buffer. Autoxidation rates were evaluated by observing the absorption spectra between 390 and 430 nm. Absorbance change in the Soret band of the oxy Mb was used for the calculation.

The coupled oxidation of oxy ferrous Mb was performed at 37 °C in 50 mM sodium phosphate buffer, pH 7.0, containing ascorbate (1 mM). The rate constants were determined on the basis of absorbance changes at an isosbestic point between the oxy- and CO-Mb.

Electrochemistry. For the reduction potential measurements of Fe^{3+}/Fe^{2+} couple, all of the samples were degassed by argon and further by the glucose (5 mM), glucose oxidase, and catalase system in 50 mM sodium phosphate (pH 7.0).[15] The ferric Mb was then reduced to the ferrous state by the irradiation of a white lamp, in the presence of EDTA

(11) Ozaki, S.; Matsui, T.; Watanabe, Y. *J. Am. Chem. Soc.* **1996**, *118*, 9784−9785.
(12) Ozaki, S.; Matsui, T.; Watanabe, Y. *J. Am. Chem. Soc.* **1997**, *119*, 6666−6667.
(13) Murakami, T.; Morishima, I.; Matsui, T.; Ozaki, S.; Watanabe, Y. *J. Chem. Soc. Chem. Commun.* **1998**, 773−774.
(14) Springer, B. A.; Egeberg, K. D.; Sliger, S. G.; Rohlfs, R. J.; Mathews, A. J.; Olson, J. S. *J. Biol. Chem.* **1989**, *264*, 3057−3060.

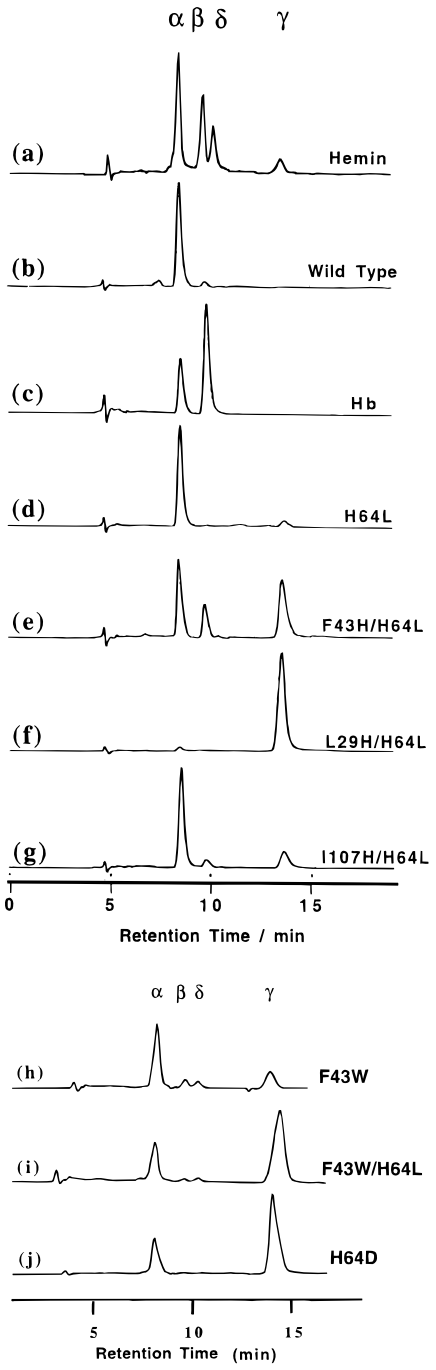

Figure 2. HPLC analysis of product isolated from the coupled oxidation of Mbs with ascorbate at 37 °C for 3 h: (a) four biliverdin isomers and products extracted from (b) wild-type Mb, (c) Hb, (d) H64L, (e) F43H/H64L, (f) L29H/H64L, (g) I107H/H64L, (h) F43W, (i) F43W/H64L, and (j) H64D Mbs.

(1 mM). Methylene blue, thionine, and phenosafranine were used as mediators. The reduction potential and the optical absorption spectra were measured at the same time at 25 °C by a Metrohm 744 pH meter equipped with Metrohm AG 9100 Herisau electrode and by a Perkin-Elmer Lambda 19 spectrometer, respectively. Sample concentration was ca. 5 μM.

The midpoint potential (E_0) of Mb was obtained from the plot of the monitored electrode potential (E_h) against the percentage of reduced Mb estimated from the absorbance change at the Soret band of the oxidized Mb by using the following Nernst equation:

$$E_h = E_0 + (RT/\nu F) \log\{[\text{oxidized Mb}]/[\text{reduced Mb}]\}$$

where ν and F denote number of electrons involved in the redox reaction and Faraday constant, respectively. The midpoint potential was corrected by utilizing methylene blue (−11 mV) as a standard. The potential was referred to the standard hydrogen electrode.

Biliverdin Extraction and HPLC Analysis. To a 250 μL solution of the ferric complexes of wild-type, mutant Mbs or human Hb (40 μM) in 50 mM sodium phosphate buffer (pH 7) was added sodium ascorbate (2 mg), and the resulting solution was incubated at 37 °C for 3 h. Extraction of biliverdin regioisomers was performed as previously reported.[16] The products dissolved in methanol were loaded on a high-pressure liquid chromatograph (Waters 600) equipped with Waters 741 data module and TOSOH CO-8020 column oven. A reverse phase HPLC column (Whatman Partisil 5 ODS-3) was employed at 40 °C at a flow rate of 0.7 mL/min with 75:25 (v/v) methanol−25 mM ammonium phosphate buffer (pH 3.5) and detected at 380 nm.

A mixture of four biliverdin regioisomers was prepared from protoheme IX according to the method reported.[4b]

Results

HPLC Analysis of the Coupled Oxidation Products. The regiospecificity of the coupled oxidation of Mb mutants has been examined by incubating the samples with ascorbate in aerobic condition at 37 °C for 3 h. Since Fe^{3+}−biliverdin is known to be formed instead of a free form of biliverdin[17] in the coupled oxidation with ascorbate, we have converted Fe^{3+}−biliverdin·Mb complex to biliverdin by the treatment with acetic acid and HCl. A HPLC system separates the four biliverdin regioisomers derived from heme.

Figure 2a shows a HPLC trace for the products of the coupled oxidation of hemin. Peaks at the retention times of 8.4, 9.8, 10.4, and 13.6 min correspond to the four biliverdin isomers because each peak shows absorption maxima around 380 and 650 nm, typical of biliverdin. An isomer having retention time of 8.4 min is identified as the α-isomer by comparison with authentic biliverdin IXα and the product of wild-type Mb (Figure 2b) which affords mainly biliverdin IXα. Figure 2c exhibits two oxidation products from human Hb (8.4 and 9.8 min). Since human Hb is known to give the α- and β-isomers in the coupled oxidation, the peak at 9.8 min is identified as biliverdin IXβ.[18] We have assigned the peak at 13.6 min to the γ-isomer on the basis of the results reported previously.[18] Therefore, the elution sequence of the isomers of biliverdin is α- (8.4 min), β- (9.8 min), δ- (10.4 min), and γ-isomer (13.6 min).[19]

Replacement of the distal histidine with a nonpolar leucine residue does not alter the major product; however, a negatively charged asparatate residue at the 64 position increases the ratio of γ-biliverdin IX to 69% (Table 1). Interestingly, the L29H/H64L mutant gives γ-isomer almost exclusively. Relocation of the distal histidine at the 43 and 107 positions also increases

(15) Makino, R.; Uno, T.; Sakaguchi; Ishimura, Y. *Oxygenase and Oxygen Metabolism*; Makino, R.; Uno, T.; Sakaguchi; Ishimura, Y., Ed.; Academic Press: New York, 1982; pp 467−477.

(16) Brown, S. B.; Docherty, J. C. *Biochem. J.* **1978**, *173*, 985−987.

(17) Yoshida, T.; Ishikawa, K.; Sato, M. *Eur. J. Biochem.* **1991**, *199*, 729−733.

(18) Hirota, K.; Yamamoto, S.; Itano, H. A. *Biochem. J.* **1985**, *229*, 477−483.

(19) To verify the elution order, we esterified the free acids of biliverdin isomers in methanolic 5% H_2SO_4 at 4 °C for 16 h. The biliverdin methyl esters were extracted with chloroform, and the sample was injected on Tosoh TSK Silica 60 (4.6 mm × 25 cm). The elution was monitored at 375 nm. Conditions: mobile phase, CH_2Cl_2:MeOH:H_2O (99:0.9:0.1); flow rate, 1.5 mL/min; column temperature, 40 °C. The retention times for α-, β-, γ-, and δ-biliverdin methyl esters were 10.6, 9.2, 12.2, and 17.3 min, respectively. The order of elution was the same as reported by R. D. Rasmussen et al.: *Anal. Biochem.* **1980**, *101*, 66−74. Furthermore, the ratio of esterified biliverdin isomers determined by the method was essentially the same as the value for free acids obtained by the procedure described in the text.

Scheme 2. Reaction Mechanism of the Coupled Oxidation of F43H/H64L and I107H/H64L Mbs

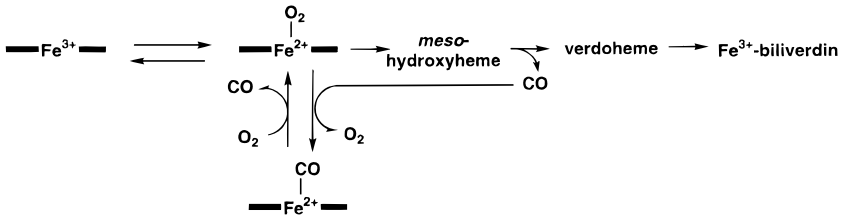

Table 1. Ratio of Four Biliverdin Isomers Produced by the Coupled Oxidation of Mbs[a]

	α	β	γ	δ
WT	95	5	trace	trace
H64L	94	trace	6	trace
L29H/H64L	3	trace	97	trace
F43H/H64L	40	16	44	trace
I107H/H64L	72	6	22	trace
F43W/H64L	33	3	61	3
F43W	57	10	25	8
H64D	31	trace	69	trace

[a] Ratio of the peak area.

the amount of γ-isomer to 44 and 22%, respectively. It appears that polar or charged residues in the heme pocket, except for the distal histidine of the wild type (His-64), somehow facilitate the formation of γ-biliverdin, but His-64 in wild-type Mb sterically blocks the γ-meso position to prevent γ-isomer production (Figure 1). Although a tryptophan side chain is not polar, the replacement of Phe-43 with Trp also increases the ratio of γ-isomer with respect to the H64L mutant. The nitrogen of the indole ring might function as a hydrogen donor in the interaction with the terminal oxygen atom of the oxy intermediate (Scheme 1).

Monitoring of the Coupled Oxidation by Electronic Absorption Spectroscopy. The coupled oxidation of the Mb mutants employed in this study exhibits four different reaction profiles: (1) ferric → oxy → Fe^{3+}−biliverdin (wild type), (2) ferric → oxy → CO complex → Fe^{3+}−biliverdin (F43H/H64L and I107H/H64L Mb), (3) ferric → Fe^{3+}−biliverdin (L29H/H64L and F43W Mb), (4) ferric → CO complex → Fe^{3+}−biliverdin (H64L, F43W/H64L, and H64D Mb). The accumulation of the CO complex in some of these mutants appears to be due to the product inhibition. Carbon monoxide produced in the reaction binds to the ferrous heme iron, and the slow release of CO followed by the oxygen rebound leads to the further heme degradation (Scheme 2).

On the basis of the spectral changes, the rate constants for the oxy Mb formation and its decay are 3.0×10^{-2} and 5.1×10^{-3} min^{-1}, respectively. In the initial stage of coupled oxidation, the oxy species of the F43H/H64L and I107H/H64L mutant are generated by 10- and 30-fold faster than that of wild-type Mb, respectively (Table 2).

To examine the heme degradation of the oxy complex of Mb, we have monitored the time-dependent absorbance changes at 417 nm for wild-type, F43H/H64L, and F43W Mb and 419 nm for the I107H/H64L mutant. Preparations of the oxy complexes of L29H/H64L, F43W/H64L, H64L, and H64D Mb were precluded because of rapid autoxidation of the oxy form. The red shift of the Soret during the coupled oxidation of oxy complexes of F43H/H64L and I107H/H64L Mb indicates the CO complex formation, and the dissociation of CO and the rebound of O_2 must be involved for the further heme degradation. The Fe^{3+}−biliverdin formation from the oxy complexes of F43H/H64L, I107H/H64L, and F43W Mb was found to be

Table 2. Rate Constant for the Formation of Oxy Mb in the Initial Stage of the Coupled Oxidation (k_{O_2}) and Autooxidation of Oxy Mb (k_{ox})

	rate constant (min^{-1})	
Mb	k_{O_2}[a]	k_{ox}
wild-type	3.0×10^{-2}	3.0×10^{-3}
F43H/H64L	3.4×10^{-1}	7.4×10^{-2}
I107H/H64L	9.3×10^{-1}	7.6×10^{-2}

[a] Rate constants determined based on absorbance change at the Soret band of the ferric Mb until 30, 11, and 4 min after the addition of ascorbate at 37 °C to wild-type, F43H/H64L, and I107H/H64L Mbs, respectively.

Table 3. Rate Constants for the Coupled Oxidation of Oxy Ferrous Mb in 50 mM Sodium Phosphate Buffer, pH 7.0, at 37 °C

Mb	rate constant (min^{-1})	
wild-type	3.2×10^{-3}	
F43H/H64L	4.5×10^{-2}	3.8×10^{-3}
I107H/H64L	7.0×10^{-2}	7.0×10^{-3}
F43W	9.9×10^{-2}	2.0×10^{-3}

fitted by two single-exponential functions as applied before,[20] while the kinetics for the wild type was fitted as a single-exponential process (Table 3). It is clear that the molecular oxygen bound to the heme iron is efficiently activated and used for the heme degradation.

The rate constants of autoxidation were determined on the basis of changes in absorbance of the Soret band of the oxy myoglobins at 37 °C. All spectra show the conversion of the oxy form to ferric Mb with clear isosbestic points. First-order autoxidation for the wild type and mutants are shown in Table 2. The oxy F43H/H64L and I107H/H64L Mbs are autooxidized over 20-fold faster than wild-type Mb, while the autoxidation rate for H64L Mb is known to be higher than that of wild-type Mb by ∼200-fold.[21]

Reduction Potential Measurement of Fe^{3+}/Fe^{2+} Couple. The reduction potentials of the Fe^{3+}/Fe^{2+} couples for F43H/H64L, I107H/H64L, and H64L Mb are determined to be 88 ± 4, 60 ± 2, and 83 ± 4 mV, respectively. The values are greater than the corresponding redox potential of wild-type Mb (52 ± 2 mV) under the same conditions. Interestingly, the E_0 value of the L29H/H64L mutant (−22 ± 3mV) is similar to the redox potential of V67A/V68S Mb (−23 mV), of which the active site is polar.[20]

Discussion

We have observed the changes in the regioselectivity of the coupled oxidation process utilizing active site Mb mutants. Although heme in L29H/H64L and H64L Mbs is almost regiospecifically oxidized to γ- and α-biliverdin, respectively, the other mutants provide mixtures of isomers. The complete

(20) Hildebrand, D. P.; Tang, H.-l.; Luo, Y.; Hunter, C. L.; Smith, M.; Brayer, G. D.; Mauk, A. G. *J. Am. Chem. Soc.* **1996**, *118*, 12909−12915.
(21) Quillin, M. L.; Arduini, R. M.; Olson, J. S.; Phillips, G. N., Jr. *J. Mol. Biol.* **1993**, *234*, 140−155.

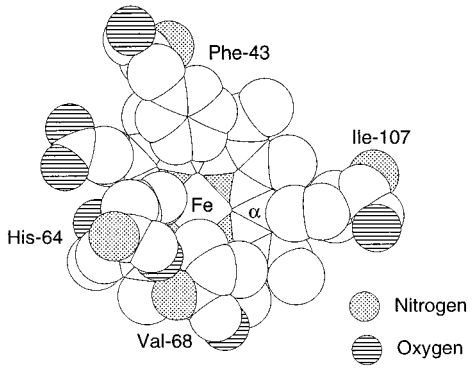

Figure 3. X-ray crystal structure of heme pocket of ferric wild-type Mb. Val-68, Phe-43, and His-64 are shown.

rationalization is complicated, but the steric hindrance, hydrogen bond interaction, and polarity of the active site as well as an electronic effect of the porphyrin would help at least partly in understanding the regioselective oxidation of protoporphyrin IX by Mb mutants.

The hydrogen bond between the distal histidine and molecular oxygen bound to the heme iron is known to play a crucial role in the stabilization of oxy Mb. The X-ray crystal structure of oxy Mb indicates that the molecular oxygen bound to heme iron is forced to bend toward pyrrole ring A in the wild type.[10] Since the β-, γ-, δ-*meso* positions are protected (Figure 3), the regiospecific opening of the tetrapyrrole macrocycle at the α-*meso* position in wild-type Mb is dominant (Table 1). Thus, the α specificity for the wild type would be rationalized by the bound oxygen molecule and/or steric effects.

Somewhat surprisingly, the elimination of His-64 did not alter the regioselectivity, i.e., the H64L mutant also gives α-biliverdin as the major product with only a small amount of γ-isomer even though the γ-*meso* position is exposed (Table 1, Figure 3). The α-*meso*-carbon might be much more reactive than the γ-*meso*-carbon. However, the orientation of oxygen molecule bound to the heme iron is not known due to the lack of X-ray crystal structure for oxy H64L Mb, and the α specificity for the mutant is not clear at the moment.

H64L Mb could be a good starting hemoprotein to elucidate effects of the distal histidine on the coupled oxidation. The introduction of a histidine residue at the 29, 43, and 107 positions of H64L Mb increases the ratio of γ-biliverdin to 97, 44, and 22%, respectively (Table 1). We speculate that a chargeable histidine residue might induce biased polarity in the heme pocket to enhance the γ-specificity. The increase in the ratio of γ-biliverdin to 69% by the His-64 $\rightarrow$ Asp mutation supports our hypothesis (Table 1), although the mechanistic detail for the enhancement in γ-specificity under the polar environment is not known at the moment. It is surprising that the L29H/H64L mutant, where the distal histidine lies farther from the heme iron than in F43H/H64L Mb,[22] gives almost γ-biliverdin by the coupled oxidation. The close examination of the active site structure of ferric H64L/L29H Mb reveals that there are two water molecules in the heme pocket: one is a ligand of the iron, and the other is in the hydrogen bond distance with Nϵ of His-29 and the ligated water molecule.[22] The polarized water molecule might be the reason for the unexpectedly high γ-specificity for the mutant. The low redox potential of L29H/H64L Mb (−22 mV), which is similar to that of the V67A/V68S mutant (−23 mV),[20] also suggests a polar active site for the L29H/H64L mutant.

Interestingly, the Phe-43 $\rightarrow$ Trp mutation enhances the γ-specificity to 25% with respect to H64L Mb (Table 1). The mutation might perturb His-64, blocking the γ-*meso*-carbon, to open up the heme pocket. Furthermore, the elimination of His-64 from F43W Mb increases the ratio of γ-biliverdin. Since a tryptophan residue is hydrophobic, we cannot rationalize the results by biased polarity effect. Thus, we hypothesize that the hydrogen bonding interaction between the nitrogen of the indole ring and the bound-O_2 could be important for γ-regiospecificity for the F43W and F43W/H64L mutant. If this is the case, the interaction might perturb the orientation of the bound dioxygen toward the γ-*meso* carbon. However, it would be difficult to determine the crystal structures of oxygenated forms of F43W and F43W/H64L Mb due to the high rates of autoxidation.

In summary, our observation in regiospecificity for the coupled oxidation of Mb would be summarized as follows: (1) The α-*meso*-carbon is the most oxidizable because the other three *meso*-carbons are sterically blocked by Phe-43 for the β, His-64 for γ-, and Val-68 for δ-*meso*-carbon. (2) Replacement of His-64 with Leu still affords α-biliverdin, possibly due to high reactivity of the α-*meso*-carbon. (3) Introduction of a charged residue such as His or Asp in the heme pocket of H64L Mb increases the γ-specificity due to polar effect. (4) An amino acid like Trp or His can also regulate the regiospecificity by hydrogen bond interaction.

The molecular basis for the regiospecificity of heme degradation by heme oxygenase has not been completely clarified yet. ^{1}H NMR of heme oxygenase showed a similar spectrum to that of a synthetic iron porphyrin with an electron-donating substituent at α-*meso*-position and suggests electronic control.[23] The results by utilizing methylmesoheme and formylmesoheme also suggested that the regiochemistry of heme degradation by heme oxygenase could be primarily controlled by electronic rather than steric effects.[4] However, the results of coupled oxidation by the Mb mutants in this study imply that hydrogen bond interaction and polarity of the heme pocket as well as electronic effects of the porphyrin would help in understanding the regioselective heme degradation by heme oxygenase in some cases even though the mechanisms may not be the same as those in Mb.

Acknowledgment. The authors thank Dr. Satoshi Takahashi for his helpful discussions. This study was supported by a Grant-in-Aid for Scientific Research on Priority Areas, Molecular Biometallics, by the Ministry of Education, Science, Sports and Culture (Y.W. and I.M.).

Supporting Information Available: Figure giving absorption spectral changes during the coupled oxidation of wild type, F43H/H64L, L29H/H64L, I107H/H64L, H64L, F43W, F43W/H64L, and H64D Mb (PDF). This material is available free of charge via the Internet at http://pubs.acs.org.

JA9834576

(22) Matsui, T.; Ozaki, S.; Liong, E.; Phillips, G. N.; Watanabe, Y. submitted for publication. The coordinates of F43H/H64L and L29H/H64L Mb are deposited at the Protein Data Bank.

(23) (a) Hernández, G.; Wilks, A.; Paolesse, R.; Smith, K. M.; Ortiz de Montellano, P. R.; La Mar, G. N. *Biochemistry* **1994**, *33*, 6631−6641. (b) Tan, H.; Simonis, U.; Shokhirev, N. V.; Walker, F. A. *J. Am. Chem. Soc.* **1994**, *116*, 5784−5790.